2. Beek, W. J., and C. A. P. Bakker, *Appl. Sci. Res.*, **A10**, 241 (1961).
3. Butler, R. M., and A. C. Plewes, *Chem. Eng. Progr. Symp. Ser. No. 10*, **50**, 121 (1954).
4. Byers, C. H., and C. J. King, *U.S. Atomic Energy Comm. Rept. UCRL-16535* (1966).
5. ———, *J. Phys. Chem.*, **70**, 2499 (1966).
6. ———, *AIChE J.*, 13, 628-636 (1967).
7. Goodgame, T. H., and T. K. Sherwood, *Chem. Eng. Sci.*, **3**, 37 (1954).
8. Goodridge, Francis, and G. Gartside, *Trans. Inst. Chem. Engrs.*, **43**, T62 (1965).
9. *Ibid.*, T74.
10. Hatch, T. F., and R. L. Pigford, *Ind. Eng. Chem. Fundamentals*, **1**, 209 (1962).
11. Higbie, Ralph, *Trans. Am. Inst. Chem. Engrs.*, **31**, 365 (1935).
12. Jaymond, M., *Chem. Eng. Sci.*, **14**, 126 (1961).
13. King, C. J., *AIChE J.*, **10**, 671 (1964).
14. ———, *Ind. Eng. Chem. Fundamentals*, **4**, 125 (1965).
15. Lewis, W. K., *Mech. Eng.*, **44**, 445 (1922).
16. Merson, R. L., and J. A. Quinn, *AIChE J.*, **11**, 391 (1965).
17. Rossi, C., E. Bianci, and A. Rossi, *J. Chim. Phys.*, **55**, 99 (1958).
18. Scriven, L. E., and R. L. Pigford, *AIChE J.*, **4**, 439 (1958).
19. *Ibid.*, **5**, 397 (1959).
20. Tang, Y. P., and D. M. Himmelblau, *ibid.*, **9**, 630 (1963).
21. ———, *Chem. Eng. Sci.*, **18**, 143 (1963).
22. van Krevelen, D. W., and P. J. Hoftijzer, *Rec. Trav. Chim.*, **68**, 221 (1949).
23. Westkeamper, L. E., and R. R. White, *AIChE J.*, **3**, 69 (1957).
24. Whitman, W. G., *Chem. Met. Eng.*, **29**, 146 (1923).

*Manuscript received July 13, 1966; revision received October 13, 1966; paper accepted October 14, 1966. Paper presented at AIChE Detroit meeting.*

# The Streaming Potential Fluctuations in a Turbulent Pipe Flow

**HENRY LIU**

**University of Missouri, Columbia, Missouri**

**Accompanied by a brief theoretical consideration, the results of an experimental study of the streaming potential fluctuations in turbulent pipe flows of distilled water are presented. The dependence of the streaming potential fluctuations on turbulent velocity fluctuations and other parameters as indicated by the theory is determined from the experimental data. Information on the characteristics of turbulent velocity fluctuations in the viscous sublayer near a pipe wall have been inferred from the data.**

It is well known that surface preferential adsorption of ions causes an electric double layer to exist at any solid-liquid interface (*1* to *4*). For water and solutions thereof, the diffuse layer, which is the outer part of the double layer, extends a distance of the order of 100 Å. or less from the wall (the distance depends on the concentration and valence of the ions in the solution, the dielectric constant, and the temperature of the fluid). When the liquid is forced to flow through a capillary tube, the transport of the diffuse-layer charge by the flow creates a convective electric current in the flow direction. A conduction current of opposite direction develops and a potential difference $\psi_s$ (the streaming potential) arises along the tube. The equation of the streaming potential for a steady laminar flow, as derived by Helmholtz (*5*) and Smoluchowski (*6*), is

$$\psi_s = \frac{\epsilon_0 \kappa \zeta \Delta p}{\mu \sigma_0}$$

Note that the equation is given here in its mks unit form.

In 1928 Reichardt (*7*) showed experimentally that this equation is also valid for turbulent flow, provided that $\Delta P$ and $\psi_s$ represent, respectively, the time averages of the pressure and potential differences along the tube. He also predicted that a fluctuating component of the streaming potential would exist in a turbulent flow, although his instrument was not sensitive enough to detect it. Bocquet (*8*) actually measured such a fluctuation in a pipe. He also proposed the idea of utilizing the phenomenon to study turbulence near a wall. Boumans (*9*), Gavis and Koszman (*10* to *13*), and many others have studied electrokinetic phenomena in turbulent flow of low conductivity fluids, with major interests in the mean rather than the fluctuating quantities of the electrokinetic flow. A series of studies of the electrokinetic potential fluctuations in water has been made by Binder (*14*), Chuang (*15*), Duckstein (*16*), and Liu (*17*).

The purpose of this paper is to describe the theory

of streaming potential fluctuations in turbulent flow of an incompressible fluid of high conductivity, and to present some experimental data collected during a study of water flowing in a circular pipe. The correlation between streaming potential fluctuations and turbulent velocity fluctuations near the pipe wall is studied, and the eddy convection velocity (disturbance velocity) in the viscous sublayer has been measured as an application of this technique to study turbulence near the wall. In the analysis which follows, all electrical equations used are expressed in the mks unit form.

## THEORY

Consider a turbulent flow of an incompressible fluid near a solid wall. Due to the existence of turbulence, the random motion of the fluid agitates the double-layer charges and produces instantaneous convective current fluctuations in the liquid phase. Consequently, fluctuating currents due to conduction and diffusion arise. If the fluid is assumed to be an electrolyte of $N$ different kinds of ions, and if it is assumed that the valences of cations and anions in the fluid are the same and that all ions have equal diffusivity, one may obtain (*11*) a charge transport equation for the electrokinetic flow:

$$\frac{\partial \rho}{\partial t} + \mathbf{v} \cdot \nabla \rho + \frac{\sigma \rho}{\kappa \epsilon_o} = \nabla \sigma \cdot \nabla \psi + \frac{\lambda^2}{\tau} \nabla^2 \rho \qquad (1)$$

Since Equation (1) holds instantaneously in a turbulent flow, the variables $\rho$, $\mathbf{v}$, $\sigma$, and $\psi$ in the equation can be substituted by the sum of the mean and fluctuating quantities $\rho = \bar{\rho} + \rho'$, $\mathbf{v} = \bar{\mathbf{v}} + \mathbf{v}'$, $\sigma = \bar{\sigma} + \sigma'$, and $\psi = \bar{\psi} + \psi'$, respectively, to yield

$$\bar{\mathbf{v}} \cdot \nabla \bar{\rho} + \bar{\mathbf{v}} \cdot \nabla \rho' + \mathbf{v}' \cdot \nabla \bar{\rho} + \mathbf{v}' \cdot \nabla \rho' + \frac{1}{\kappa \epsilon_o} (\bar{\sigma} \bar{\rho} + \bar{\sigma} \rho' + \sigma' \bar{\rho} + \sigma' \rho') = \nabla \bar{\sigma} \cdot \nabla \bar{\psi} + \nabla \bar{\sigma} \cdot \nabla \psi' + \nabla \sigma' \cdot \nabla \bar{\psi} + \nabla \sigma' \cdot \nabla \psi' + \frac{\lambda^2}{\tau} (\nabla^2 \bar{\rho} + \nabla^2 \rho') \qquad (2)$$

for a quasisteady flow.

In Equation (2), a term $(\partial \rho'/\partial t)$ which would cause an explicit dependence of streaming potential on time has been neglected. This can be justified by a comparison of the order of magnitude of the term $(\bar{\sigma}\rho'/\kappa\epsilon_o)$ with $(\partial \rho'/\partial t)$ through the use of a Fourier integral. For water and solutions thereof, $\left| \frac{\bar{\sigma}}{\kappa \epsilon_o} \right|$ has an order of magnitude of at least $10^6$ sec.$^{-1}$. On the other hand, turbulence in an ordinary flow contains little energy when the frequency $\omega$ exceeds $10^6$ sec.$^{-1}$. Therefore it is reasonable that $\left| \frac{\bar{\sigma}}{\kappa \epsilon_o} \right| >> |i\omega|$, or, in other words, the term $(\partial \rho'/\partial t)$ is much smaller than $(\bar{\sigma}\rho'/\kappa\epsilon_o)$ and can be neglected from the equation.

Due to the complexity of Equation (2), an integrated solution of it is practically impossible to obtain. This limits the usefulness of the equation to the prediction of the variables which influence the streaming potential fluctuations. Knowing that the mean and fluctuating potentials are related to the mean and fluctuating charge densities through Poisson's equation, and that $\lambda^2/\tau$ is the diffusivity of the ions $\mathcal{D}$, one sees from Equation (2) that the streaming potential fluctuations $\psi'$ in water and solutions thereof are a function of the parameters $\bar{\mathbf{v}}$, $\mathbf{v}'$, $\bar{\rho}$, $\kappa$, $\bar{\sigma}$, $\sigma'$, $\mathcal{D}$, $\mathbf{r}$, and $B$. Functionally, this can be expressed as

$$\psi' = \phi(\bar{\mathbf{v}}, \mathbf{v}', \bar{\rho}, \kappa, \bar{\sigma}, \sigma', \mathcal{D}, \mathbf{r}, B) \qquad (3)$$

The experimental study described herein was conducted to investigate the dependence of the streaming potential fluctuations on the parameters included in Equation (3).

## EXPERIMENT

In the experiments described herein, streaming potential fluctuations produced by turbulent flow of water in a circular conduit were studied. Since measurements were made by electrodes at the pipe wall in a region of fully developed flow, no dependence of the statistical properties of the streaming potential fluctuations on position existed. However, by varying the Reynolds number, the values of $\bar{\mathbf{v}}$ and $\mathbf{v}'$ were varied and the dependence of the statistical properties of $\Psi'$ on them was studied; by using different materials for the pipe, the change of the properties of $\Psi'$ with $\bar{\rho}$ was studied; by adding salts to water and varying its concentration, the change of $\Psi'$ with conductivity of the fluid was studied.

### Test System and Liquid Used

As shown in Figure 1, the flow system was recirculating with four major parts: the reservoirs, the constant-head tank, the pump, and the main pipe lines. Water was pumped from the reservoirs to the top of the plastic constant-head tank which kept the water column 11 ft. above the main pipe line. Overflow from the tank entered a large glass bottle reservoir which was connected to the inlet of the pump through Tygon tubes. The main pipe line was connected to the bottom of the constant-head tank through a smooth entrance transition. To ensure fully developed turbulent flow, the test section, which contained electrodes on the boundary, was placed about 14 ft. downstream from the pipe inlet. The test section was made of a special 1-in. I.D. pipe 1 ft. long. It was installed with its inner surface flush with that of the main pipe line. Two brass sections, one connected immediately upstream and the other immediately downstream of the test section, were shorted to the ground to eliminate excessive electrical pickup transmitted through water from the rest of

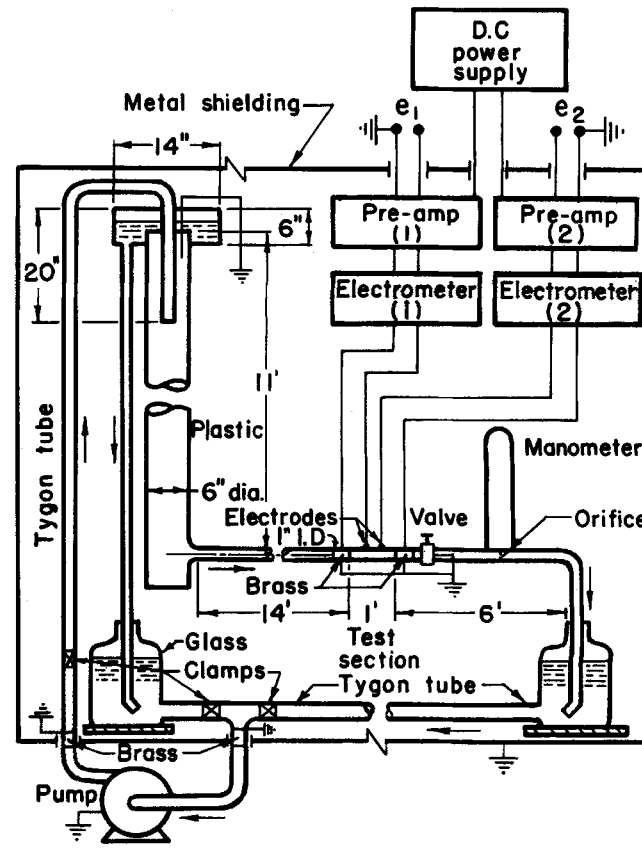


Fig. 1. Flow system and electrode circuit.

the flow system. Finally, to control and measure the discharge of the flow, a valve and an orifice meter were placed near the end of the pipe line. The flow could be varied through a range of Reynolds number between 0 and $10^5$.

Except for the case which involves the addition of salt to water, distilled water was used in all experiments because it gives a larger signal and a more stable, reproducible result than can be obtained from solutions thereof. Thus, it increases the signal-to-noise ratio for each experiment.

When distilled water was first placed into the system, its conductivity was about $1.5 \times 10^{-4}$ mho/m. Impurities from the test system combined with the fluid and after many weeks its conductivity increased to a value of about $10 \times 10^{-4}$ mho/m. At this point the fluid was drained and replaced with fresh distilled water. The conductivity of the fluid was measured before and after each test run. The water temperature was usually at 24°C. prior to the start of each run but increased to as much as 28°C. after several hours of operation. Although the increase in conductivity caused by such a change in temperature is by no means negligible, the change in signal level due to such a change was not critical. Generally, data taken at the beginning of each run compared well with those taken several hours later.

To study the influence of conductivity on the streaming potential fluctuations, different salt solutions were added to the flow to increase conductivity. The conductivities studied ranged from $2 \times 10^{-4}$ to $4 \times 10^{-2}$ mho/m. Since signal-to-noise ratio decreases as conductivity increases, it was necessary to have a grid in the pipe to generate strong turbulence and, hence, strong streaming potential fluctuations. The test electrodes were placed about 1 in. downstream from the grid.

### Electrodes and Electrode Circuit

Platinum wire was used for the electrodes because of its special inert nature. The wire size was either 0.008 or 0.013 in. in diameter, being different for different experiments. Electrodes were constructed by inserting and glueing these wires into the wall of the test section, flush with the inner surface of the pipe. Both plastic and brass pipes were used as test sections. For the brass section, the insulation between the electrodes and the test section was carefully provided.

Instead of measuring streaming potential fluctuations between two electrodes on the test section, the potential fluctuations between one electrode and the ground were measured. Thus, for the case of a plastic test section, the two grounded brass sections adjacent to the test section played the role of large electrodes, while for the case of a brass test section, the test section played the role of a large electrode since it was grounded.

As shown in Figure 1, the electrode circuit was composed of two identical electrometers and two identical preamplifiers, making it possible to measure two signals simultaneously. A battery-operated electrometer with a gain of 8 was used to provide a high input impedance (an input impedance of $10^{12}$ ohms in parallel with a small parasitic capacitance of a magnitude depending upon the type of input cables used). Its frequency response was flat from 1 to 500 cycles/sec., with approximately 5% decrease of signal amplitude at 1,000 cycles/sec.

The preamplifiers used were Tektronix type 122 differential amplifiers with a selective gain of either 100 or 1,000. They could be operated either with differential inputs or with one input-end grounded. The frequency range used for all measurements was from 0.8 to 10,000 cycles/sec. Because the signal from the electrodes (the root-mean-square value of the fluctuations) was usually less than 100 $\mu$v., it was necessary to reduce the noise level to a minimum before amplifying the signal. For this reason, the entire apparatus was housed inside the metal shield which was connected to the ground. No a.c. sources were placed inside the housing. The signal was generally amplified 8,000 times before it was sent to the output circuits located outside the shielding.

### Output Circuits

The output circuits recorded and analyzed the amplified fluctuating voltage. To detect undesirable signals, especially 60-cycle/sec. hum, an oscilloscope was always used to monitor the signal. A Brüel and Kjaer (B & K) type 2416 electronic voltmeter was used to measure the root-mean-square value of the amplified signal and a B & K type 2109 wave analyzer was used to measure the spectrum of the signal. The analyzer had a frequency response range of 15 to 32,000 cycles/sec.

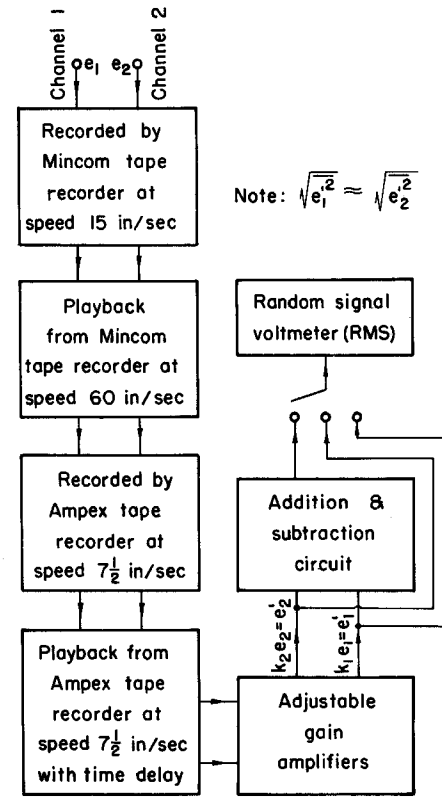


**Fig. 2. Block diagram of the procedure used in measuring longitudinal space-time correlation coefficient.**

The equipment used for the space-time correlation study is illustrated in Figure 2. Since the Ampex model 5700 tape recorder (amplitude modulation) had a poor frequency response below 50 cycles/sec., and since a large portion of energy of the signal was contained below this frequency, it was necessary to increase the signal frequency several times before it was analyzed. This was accomplished by recording simultaneously two signals with a Mincom C-100 tape recorder (frequency modulation) at a recording speed of 15 in./sec. and a frequency response from 0 to 2,500 cycles/sec. Then the recording was played back at a speed of 60 in./sec. and recorded with the Ampex tape recorder. This process increased the recorded signal frequency four times. The Ampex recorder had a movable and a fixed pickup head, making it possible to effect a time delay between the two signals. The signals were then amplified by two adjustable gain amplifiers to about the same magnitude and finally were fed into the addition and subtraction circuit to evaluate the correlation.

### Test Procedure

Before each experiment the test section was mounted to the pipe line and the entire pipe was kept filled with water for at least 24 hr. so as to allow the double layer to reach a steady equilibrium. When the flow was started for each test run, a warm-up period was allowed, which permitted air bubbles present in the fluid to disperse and the flow to become stabilized.

The conductivity and temperature of the fluid and the discharge rate were recorded before and after taking data. An average of the two readings was used to represent their values during the run.

Noise and pickup were recorded after each run. These interferences were recorded by measuring the signal in a near laminar flow. When the signal generated by the flow failed to decrease with a decrease in flow rate, it was assumed to

comprise only pickup and noise. Excessive 60-cycle/sec. pickup was easily detected by an oscilloscope, and was always minimized before taking data. Spectral distributions of the signal also provided a means of detecting the presence of 60-cycle/sec. pickup in the measurement.

## RESULTS AND DISCUSSION

### Variation of Potential Fluctuations with Reynolds Number

The variation of the streaming potential fluctuations with Reynolds number of the pipe flow was studied for electrodes of $d = 0.013$ in. on a brass and a plastic test section. The variation of the signal intensity with Reynolds number is shown in Figure 3. The result reveals a linear relationship in the higher range of Reynolds number studied and an increasing deviation from linearity with decreasing Reynolds number. The deviation from the linear relationship for small Reynolds number was at least partly due to a decrease in signal-to-noise ratio as the Reynolds number decreases. Although noise for each run was estimated in the manner described in the experimental procedure, it was not subtracted from the total signal because of some uncertainties in the estimation. The increase in the magnitude of the streaming potential fluctuations with increasing Reynolds number is due to the fact that turbulence in the diffuse layer increases with increasing Reynolds number. Streaming potential fluctuation intensities are seen to be larger in the plastic pipe than in the brass for equal Reynolds numbers (and hence, equal turbulent intensities). This difference can be attributed to the difference in $\overline{p}$ produced by the two materials and to the grounding of the brass section which produces a different boundary condition.

The variation of signal intensity with Reynolds number was also compared with Corcos' wall pressure fluctuation data (*19*) as shown in Figure 4. To make this comparison, the signal intensity measured here was multiplied by a linear scaling factor $n$. This constant $n$ was so chosen that it forces the curve of Figure 3 (for the plastic section) to fit the wall pressure fluctuation data at a Reynolds number of 95,000. The difference between the two curves in the region of low Reynolds number is prominent.

The variation of the signal spectrum with Reynolds number was recorded for the brass pipe. As shown in Figure 5, a larger fraction of the total energy of the signal

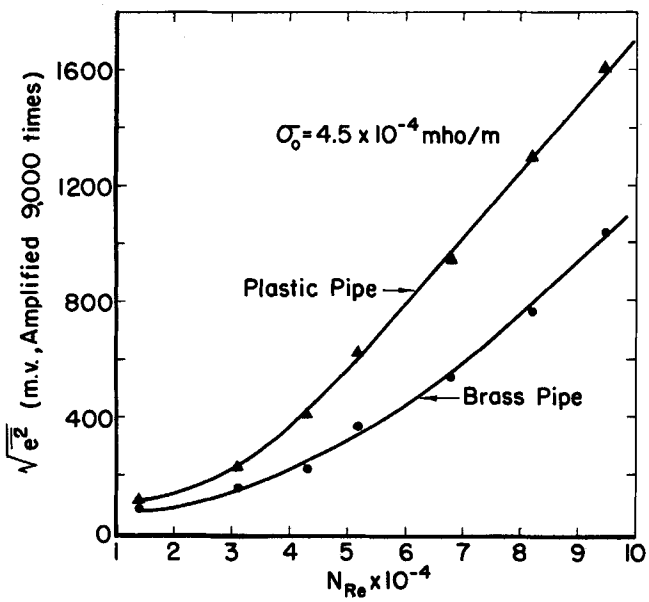


Fig. 3. Variation of signal with Reynolds number.

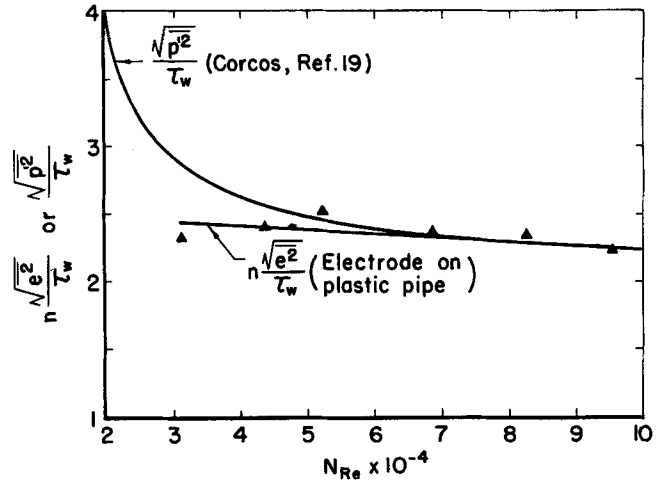


Fig. 4. Comparison of streaming potential fluctuations with wall pressure fluctuations.

is contained in the high frequency band as the Reynolds number increases. This is evidently due to the decrease in turbulence scale as the Reynolds number increases.

### Variation of Potential Fluctuations with Conductivity

The influence of fluid conductivity on the streaming potential fluctuations was studied by adding salt solutions to the flow during each run. Each time more salt solution was added to the flow, a sudden drop in signal intensity occurred. This change may be attributed to the change of conductivity of the fluid. However, following this change, the signal intensity continued to decrease slowly without any further increase in concentration. Several hours were

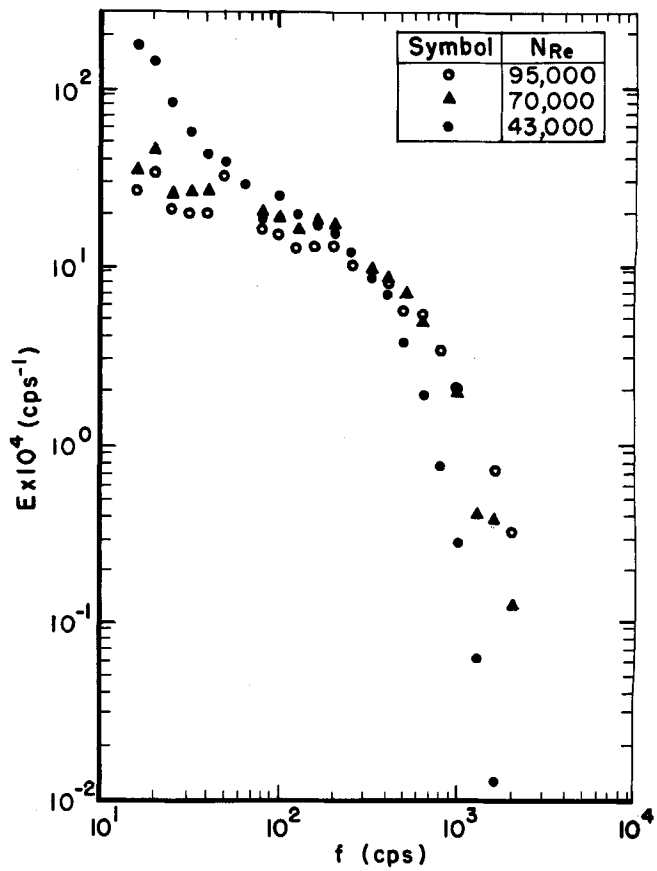


Fig. 5. Variation of normalized signal spectrum with Reynolds number (brass pipe).

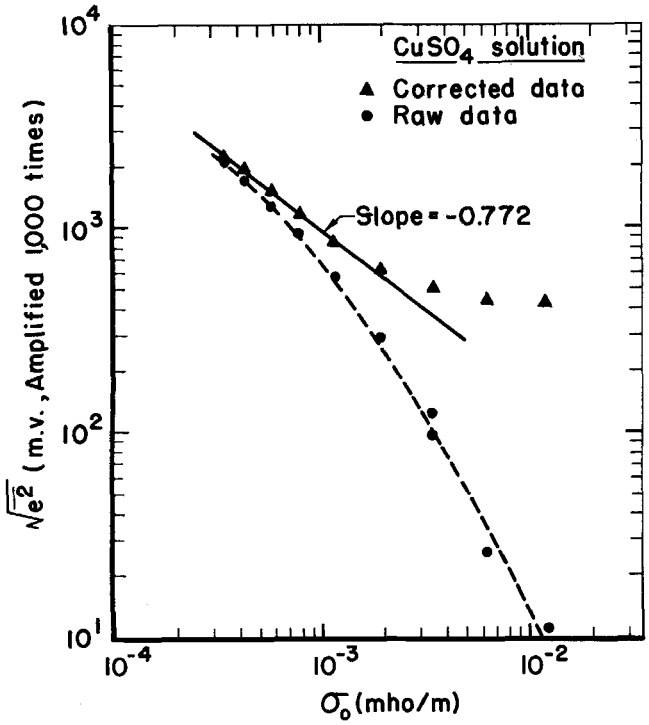


Fig. 6. Variation of signal intensity with conductivity.

required for the signal level to reach equilibrium. It is believed that this was caused by a change of adsorption and a consequent change of the mean charge distribution in the diffuse layer.

To evaluate the effect of conductivity alone, the effect due to adsorption should be excluded. It was possible to estimate this effect by recording continuously the change of signal intensity with time for each run. Since the change of signal due to adsorption had a much flatter slope than the change due to conductivity, the former effect could be estimated and subtracted from the total signal. The remaining signal is given as corrected data as is shown in Figure 6 for the case of copper sulfate solution. The raw data in the figure are the signals measured about 5 min. after each change of concentration. No effort was made to wait for the signal to stabilize after each change of concentration because of the great amount of time which would have been required.

As shown in Figure 6, the signal decreased with a slope of about 0.77 on log-log paper for lower values of $\sigma_o$. For larger conductivity, the signal-to-noise ratio becomes smaller and the slope also becomes smaller, deviating more and more from 0.77 with increasing conductivity. About the same slope and trend were found for other types of solutions. The signal spectra for different conductivities are given in Figure 7. No appreciable change of spectral shape with conductivity was found.

#### Space-Time Correlation

The space-time correlation coefficient for the signal was measured between two longitudinal electrodes with $\Delta X = 0.25$ in. (for electrodes on a plastic pipe section) and with $\Delta X = 0.04$ in. (for electrodes on a brass section). The results as plotted in Figure 8 show that the streaming potential fluctuations are convected downstream at a speed of about 0.7 to 0.8 times the bulk average velocity $U$ of the pipe flow. This result is in good agreement with Sternberg's hypothesis (*20*) and with the measurements made by Willmarth (*21*), Corcos (*19*), and many others for wall pressure fluctuations, and by Reiss, Hanratty, and Shaw (*22* to *24*) for shear stress fluctuations near the wall of a fully developed turbulent pipe flow. Therefore, the

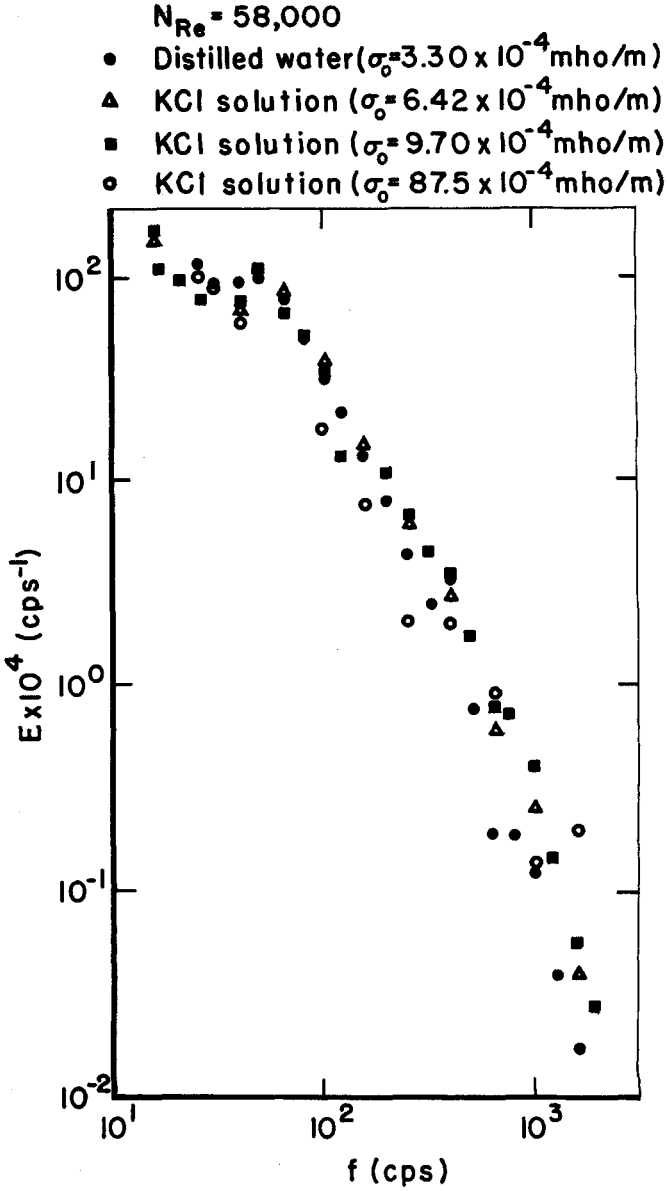


Fig. 7. Variation of normalized signal spectrum with conductivity (plastic pipe).

value of 0.7 to 0.8 $U$ obtained from this experiment not only reconfirms Sternberg's claim, but also proves that the streaming potential fluctuations, as measured in this work, were indeed caused by turbulence disturbance of the diffuse-layer charges inside the viscous sublayer of the turbulent pipe flow.

## CONCLUSION

Although a quantitative relationship between measured streaming potential fluctuations and velocity fluctuations is not known from this analysis because the functional form of Equation (3) is not known, the present experimental study provides the following qualitative information:

1. The root-mean-square value of the streaming potential fluctuations increases with increasing turbulence intensity. More specifically, it appears to increase linearly with the Reynolds number in the range from $4 \times 10^4$ to $10 \times 10^4$. This linearity breaks down for smaller Reynolds numbers at which the signal-to-noise ratio becomes poor.
2. The signal spectrum is similar to turbulence spectrum. As the mean-flow Reynolds number is increased, energy

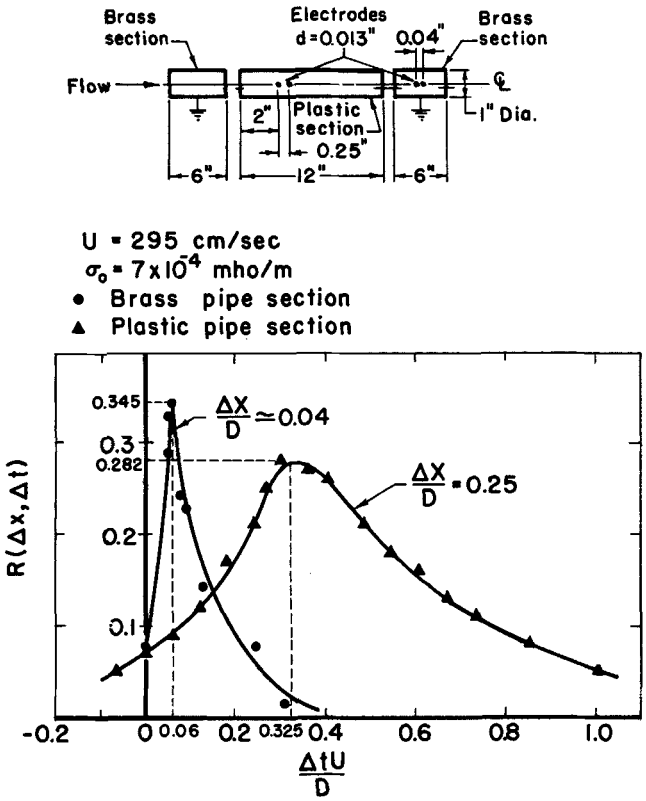


Fig. 8. Longitudinal space-time correlation.

contained in the high-frequency band increases because of the resultant decrease in the turbulence scale.

3. The signal is convected downstream at a speed of 0.7 to 0.8 times the bulk average velocity of the pipe flow, which corresponds very well to the known mean eddy convective velocity in the viscous sublayer.

4. The signal intensity decreases with increasing conductivity of the fluid.

## ACKNOWLEDGMENT

This research, which was a part of the writer's Ph.D. dissertation, was carried out at the Fluid Mechanics and Diffusion Laboratory at Colorado State University. The writer is grateful to his major professor, Dr. J. E. Cermak, and his committee member, Dr. G. J. Binder, for their guidance during the study. Financial support for the project was provided by the National Science Foundation under Grant GP 789.

## NOTATION

$B$ = arbitrary constant representing boundary conditions
$d$ = electrode diameter
$D$ = pipe diameter
$\mathcal{D}$ = diffusivity of ions
$e$ = amplified signal
$e_1$ = amplified signal of electrode 1
$e_2$ = amplified signal of electrode 2
$E$ = normalized frequency spectrum
$i$ = $\sqrt{-1}$
$k_1$ = amplification factor for $e_1$
$k_2$ = amplification factor for $e_2$
$n$ = arbitrary constant
$N$ = number of types of ions
$N_{Re}$ = Reynolds number
$P$ = pressure
$P'$ = pressure fluctuation
$\Delta P$ = pressure difference across capillary tube
$\mathbf{r}$ = position vector
$R$ = correlation coefficient
$t$ = time
$\Delta t$ = time interval
$U$ = bulk average velocity of the pipe flow
$\mathbf{v}$ = instantaneous local velocity
$\bar{v}$ = average local velocity
$v'$ = local velocity fluctuation
$\Delta x$ = longitudinal spacing between two electrodes

### Greek Letters

$\epsilon_0$ = electric constant, $8.85 \times 10^{-12}$ farad/m.
$\zeta$ = zeta potential
$\kappa$ = dielectric constant
$\lambda$ = diffuse-layer thickness
$\mu$ = dynamic viscosity
$\rho$ = instantaneous local charge density
$\bar{\rho}$ = average local charge density
$\rho'$ = fluctuation of local charge density
$\sigma$ = instantaneous local fluid conductivity
$\bar{\sigma}$ = average local fluid conductivity
$\sigma'$ = fluctuation of local fluid conductivity
$\sigma_0$ = bulk conductivity of the fluid
$\tau$ = relaxation time of the fluid
$\tau_w$ = shear stress at wall
$\psi$ = instantaneous local potential
$\bar{\psi}$ = mean value of local potential
$\psi'$ = fluctuation of local potential
$\psi_s$ = streaming potential across the tube
$\omega$ = angular frequency

## LITERATURE CITED

1. Abramson, H. A., "Electrokinetic Phenomena," J. J. Little and Ives, New York (1934).
2. Bikerman, J. J., "Surface Chemistry," 2 ed., Academic Press, New York (1958).
3. Davis, J. T., and E. K. Rideal, "Interfacial Phenomena," Academic Press, New York (1961).
4. Grahame, D. C., *Chem. Rev.*, **41**, 441 (1947).
5. Helmholtz, H. L. F. Von, *Eng. Res. Bull.*, Univ. Michigan, Ann Arbor (1951).
6. Smoluchowski, M. Von, *Eng. Res. Bull.*, Univ. Michigan, Ann Arbor (1951).
7. Reichardt, H., "Elektrische Potentiale bei Laminarer und bei Turbulenter Strömung," Georg August Univ., Goettingen (1928).
8. Bocquet, P. E., C. M. Sliepeevich, and D. F. Bohr, *Ind. Eng. Chem.*, **48**, 197 (1956).
9. Boumans, A. A., *Physica*, **23** (11), 1007 (1957).
10. Gavis, J., and I. Koszman, *J. Colloid. Sci.*, **16**, 375 (1961).
11. Gavis, J., *Chem. Eng. Sci.*, **19**, 237 (1964).
12. Koszman, I., and J. Gavis, *Chem. Eng. Sci.*, **17**, 1013 (1962).
13. *Ibid.*, 1023.
14. Binder, G. J., Ph.D. dissertation, Colorado State Univ., Fort Collins (1960).
15. Chuang, H., Ph.D. dissertation, Colorado State Univ., Fort Collins (1962).
16. Duckstein, L., Ph.D. dissertation, Colorado State Univ., Fort Collins (1962).
17. Liu, Henry, Ph.D. dissertation, Colorado State Univ., Fort Collins (1966).
18. Burgreen, D., *U.S. Aeronaut. Syst. Div. Tech. Document Rept. No. ASD-TDR-63-243* (1963).
19. Corcos, G. M., *J. Fluid Mech.*, **18**, 353 (1964).
20. Sternberg, J., *ibid.*, **13**, 241 (1962).
21. Willmarth, W. W., and C. E. Wooldridge, *ibid.*, **14**, 187 (1962).
22. Reiss, L. P., and T. J. Hanratty, *AIChE J.*, **8**, 245 (1962).
23. *Ibid.*, **9**, 154 (1963).
24. Shaw, P. V., and T. J. Hanratty, *ibid.*, **10**, 475 (1964).

*Manuscript received July 14, 1966; revision received October 28, 1966; paper accepted October 28, 1966.*